HEAT TRANSFER CORRELATION FOR A REFRIGERANT MIXTURE IN A VERTICAL HELICAL COIL EVAPORATOR

by

Raja BALAKRISHNAN, Joseph Sekhar SANTHAPPAN, and Mohan Lal DHASAN

Original scientific paper
UDC: 621.5.04:536.24
DOI: 10.2298/TSCI0904197R

The flow boiling heat transfer study of R-134a/R-290/R-600a refrigerant mixture is carried out in a vertical helical evaporator test section. The test section is immersed in an agitated ethylene glycol-water bath maintained at constant temperature. An aluminum test section with a height of 0.22 m, tube inside diameter of 6.35 mm, outside diameter of 8 mm and coil length of 8 m is used. The influences of various operating parameters such as evaporating temperature, bath temperature, and refrigerant composition on the heat transfer coefficient are investigated experimentally. Using the same experimental results the shell side flow boiling heat transfer coefficient correlation in helical evaporator is also evolved.

Key words: *flow boiling, helical coil, heat transfer coefficient, R-134a, M09*

Introduction

The alarming needs to phase out chlorofluorocarbons (CFC) [1] and the subsequent research efforts have recommended R-134a, hydrocarbons, and hydrocarbon blends as prominent substitutes for R-12 [2-8]. The study conducted on R-134a in existing R-12 systems revealed that the coefficient of performance (COP) of R-134a is 2-15% lower than that of R-12 [3, 4]. Further, to retrofit with R-134a in a R-12 system, suitable changes in capillary length and compressor swept volume are required. Moreover, the higher polarity of R-134a has poor solubility with mineral oil, which is a non-polar lubricant [5]. Thus, without suitable changes in either the compressor and/or other components, R-134a cannot be treated as a drop-in substitute for R-12. The matching oil for R-134a is POE (Polyol ester) oil, which possesses a hygroscopic nature and may cause moisture entry into the circuit during service and maintenance operations. Even though hydrocarbons and their blends are miscible with mineral oil and more energy efficient than R-134a and R-12 [6-8], their flammable nature has caused concerns. Moreover, in many countries the permitted charged quantity of hydrocarbons in refrigerators and supermarket freezer appliances are restricted. Hence, it is prudent to look for a refrigerant – oil pair that has no service issues and can circumvent the above-mentioned quantity restriction.

Janssen *et al*. [9] have reported the oil miscibility and oil return to the compressor casing is possible by adding hydrocarbon to R-134a. Based on this, Sekhar *et al*. [10, 11] experimented with real-time appliances, and reported that adding 7%, 9%, and 11% of hydrocarbon blend, which is 54.8% of R-600a and 45.2% of R-290, to R-134a, made the resultant zeotropic mixture termed M07, M09 and M11, respectively, work well with mineral oil with enhanced performance. It is reported that M09 (R-134a/R-290/R-600a of 91%/4.068%/4.932% by mass) gives better performance among those and suggested that the same can be used as a drop-in-substitute for R-12. Recently, Raja *et al*. [12] performed flow boiling heat transfer experiments on M09 in horizontal tubes. However, complicated shaped like helical coil evaporators are frequently used in non-typical chillers and freezers. Therefore, suitable correlations are required to design the evaporators with commendable energy efficiency. Significant quantum of work on in-tube flow boiling heat transfer correlation for straight tubes are available in the published literature [13-17]. Further, there many sources are available for single-phase heat transfer in helical tubes [18-21]. However, only limited references are available for other configurations such as helical coils [22-24]. In this paper, the experimental study on flow boiling heat transfer M09 is presented and the heat transfer coefficients for the conditions prevailing in the evaporator of domestic refrigerators and freezers in vertical helical evaporator test section is presented. Based on the experimental data suitable correlation for M09 for vertical helical evaporators is also developed.

Test facility

The schematic lay-out of the test facility used in this investigation is shown in fig. 1. The test facility is a non-typical experimental bench, to mimic condition prevailing in a typical 165-litre single evaporator domestic refrigerator. The facility consists of an aluminum-evaporator test section, which is 0.22 m in height, 6.35 mm of inner diameter, 8 mm of outer diameter and 8 m of coil length, which is wound into 18 coils. Since the mixture is zeotropic in nature, to measure the temperature distribution along the evaporator coil 18 PT100-RTD temperature sensors are suitably fixed along the height of the coil. The test section placed inside a secondary refrigerant calorimeter, which is used is a double walled vessel of 250 mm outer diameter and 250 mm height that was well insulated with 65 mm poly urethane foam (PUF) in between walls and 12 mm thermo-rex on the exterior. Ethylene glycol is used as secondary refrigerant in the calorimeter. To vary the temperature of the secondary refrigerant and the heat duty, a heater is fixed suitably inside the bath. The heater load can be varied with the help of a dimmerstat, and a wattmeter is provided to measure the heater load. A stirrer is provided to maintain uniform temperature in the bath. Five temperature sensors are strategically fixed inside the calorimeter to check the uniformity of the temperature in the bath. The heat infiltration study revealed that for the entire range of calorimeter temperature for a standard ambient temperature of 32 °C, and the maximum infiltration is ensured to be less than 5% of the evaporator capacity (Bureau of Indian Standards no. 1496). The temperature and pressure sensors have both ±0.15 °C and ±0.15% accuracy, respectively. All the temperature sensors are connected to a data logger to continuously record the temperatures. The refrigerant flow rate is also measured for all test conditions. The

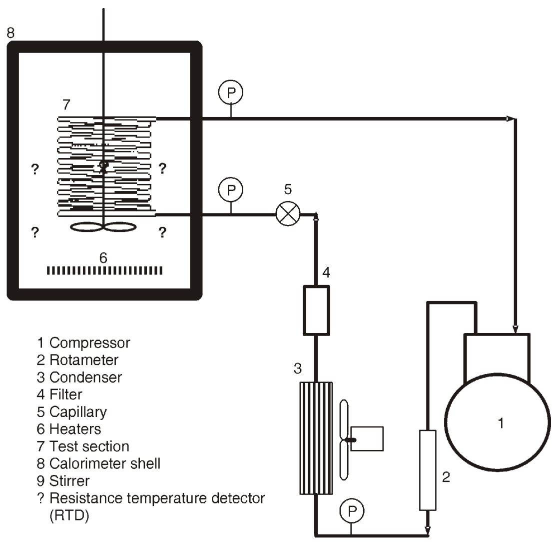

Figure 1. Schematic lay-out of the experimental set up

experiments are conducted for the calorimeter temperatures of –20, –15, –10, –6, and –4 °C. The heat load is varied from 50 W to 130 W in order to achieve these temperatures at steady-state conditions. The temperature and pressures across the test section are observed for each condition.

Data reduction

It is important to find the point along the coil length at which the dryness fraction becomes one ($x = 1$). This is not straight forward in test sections immersed in constant temperature bath. Therefore, an indirect iterative method is used to find the length. Initially, the pressure drop in the portion of helical coil, after attaining saturated vapor state is considered to be negligible. The enthalpy of the refrigerant at the exit of the test section is calculated based on the test section's measured exit pressure p_{r2} and the refrigerant exit temperature t_{r2}. Hence, the change in enthalpy of refrigerant due to two-phase flow inside the helical coil is:

$$\Delta i_{tp} = i(p_{r2}, x = 1) - i(p_{r1}, x_{r1}) \tag{1}$$

The heat taken for the phase change process (Q_{tp}) in the helical coil is calculated by subtracting the heat taken away by the superheated vapor ($m \cdot \Delta i_{sh}$) from the actual heat supplied (Q_{sh}):

$$\Delta i_{sh} = i(p_{r2}, t_{r2}) - i(p_{r2}, x = 1) \tag{2}$$

where

$$Q_{sh} \quad (\dot{m} \;\; \Delta u_{sh})$$

Therefore two-phase heat load from the actual supplied load is:

$$Q_{tp} \quad Q_{sup} \quad (\dot{m} \;\; \Delta i_{sh}) \tag{3}$$

The actual two-phase length of the helical coil is calculated as:

$$L_{tp} \quad \frac{L}{Q_{sup}} Q_{tp} \tag{4}$$

The coil length in which superheating took place is:

$$L_{sh} = L - L_{tp} \tag{5}$$

Based on this L_{sh}, the pressure drop (Δp_{sh}) due to superheated refrigerant is calculated using [23]

$$\Delta p_{sh} \quad \frac{fcL_{sh} \rho_g u_g^2}{8 d_i} \tag{6}$$

where

$$fc \quad 2.552 \, \mathrm{Re}_v^{0.15} \; \frac{d_i}{D}^{0.51}$$

Based on Δp_{sh} a saturated pressure (p_{r2sat}) at $x = 1$ is calculated from:

$$p_{r2sat} = p_{r2} + \Delta p_{sh} \tag{7}$$

The variation of pressure with respect to dryness fraction in the two-phase length (L_{tp}) of the helical coil is then estimated using the correlation [23] for frictional pressure drop. The two-phase pressure drop Δp_{tp} is subdivided into definite number of sections, and cumulatively substituting the sectional pressure drop in eqs. (8) and (9), the dryness fraction corresponding to pressure drop is iteratively calculated and the variation of pressure with respect to variation in the dryness fraction, indirectly the length, is also digitized:

$$\Delta p_{\mathrm{tp}} \quad \Delta P_{\mathrm{L}} \psi_1 \psi \quad 1 \quad x \frac{\rho_{\mathrm{L}}}{\rho_{\mathrm{g}}} \quad 1 \tag{8}$$

where

$$\Delta P_{\mathrm{L}} \quad \frac{fcL_{\mathrm{tp}} \rho_{\mathrm{L}} u_{\mathrm{L}}^2}{8 d_{\mathrm{i}}} \tag{9}$$

$$fc \quad 2.552 \, \mathrm{Re}_{\mathrm{L}}^{0.15} \quad \frac{d_{\mathrm{i}}}{D}^{0.51} ; \quad \psi_1 \quad 142.2 \quad \frac{p}{p_{\mathrm{cr}}}^{0.62} \quad \frac{d_{\mathrm{i}}}{D}^{1.04} ; \quad \psi \quad 1 \quad \frac{A}{B} \quad \text{for } G \quad 1000;$$

$$A \quad x(1 \quad x) \quad \frac{1000}{G} \quad 1 \quad \frac{\rho_{\mathrm{L}}}{\rho_{\mathrm{g}}}; \quad B \quad 1 \quad (1 \quad x) \quad \frac{\rho_{\mathrm{L}}}{\rho_{\mathrm{g}}} \quad 1$$

Next is to find the wall superheat, which is required to find the heat transfer coefficient ($h = q_{\mathrm{tp}}/\Delta T_{\mathrm{w}}$). It is postulated that the global heat transfer in a flow boiling process is the net effect of nucleate boiling and convective vaporization processes [18-21]. In the former process, the heat transfer is predominantly due to bubble formation and the magnitude of the heat transfer coefficient is directly proportional to the heat flux. In the latter one, the heat transfer process is due to convective vaporization of liquid at the liquid-vapor interface and the heat transfer coefficient is proportional to the mass flux. It has been pointed out that the regions pertaining these mechanisms can be demarcated by identifying the location where the nucleate boiling gets suppressed [18-21]. Due to the presence of a capillary expansion prior to the inlet of the helical coil, in the present work, it is estimated that the refrigerant enters the test section with a higher dryness fraction say 0.3. Based on the L_{tp} and Q_{tp} the heat flux (q) is calculated and the relation to find the wall super heat cited in Wattelet *et al*. [15]. The saturation temperature or the bubble temperature is calculated from the digitized profile of pressure values against dryness fraction from which variation of T_{w} along the L_{tp} was calculated:

$$q \quad \frac{k_1 (T_{\mathrm{w}} \quad T_{\mathrm{sat}})^2}{4B} \tag{10}$$

where

$$B \quad \frac{2\sigma T_{\mathrm{sat}}}{(\rho_1 \quad \rho_{\mathrm{g}}) i_{\mathrm{fg}}}$$

Finally, the two-phase heat transfer coefficient for every subsection is calculated from ($h_{\mathrm{ts}} = q_{\mathrm{tp}}/\Delta T_{\mathrm{w}}$), where q_{tp} is based on the two-phase heat load (Q_{tp}) and for the surface area calculated from two-phase length (L_{tp}). A length averaged heat transfer coefficient is correlated against dimensionless number such as Dean number (De) and Pierre boiling number ($\mathrm{K_f}$). The subsection of the helical coil along with the constant temperature bath is considered as small heat exchangers and the logaritmic mean temperature difference values are obtained. The overall heat transfer coefficient (U) is calculated corresponding to the heat load for every subsection.

$$\frac{1}{U} \quad \frac{1}{h_{\mathrm{ss}}} \quad \frac{\ln \dfrac{d_{\mathrm{o}}}{d_{\mathrm{i}}}}{2\pi k_{\mathrm{tube}} \Delta L_{\mathrm{tp}}} \quad \frac{1}{h_{\mathrm{ts}}} \tag{11}$$

$$\text{subsection}$$

Correlation development

Sami *et al*. [26] performed flow boiling heat transfer experiments R502, R507, R407B, R32/R125/R134a/R143a blend on horizontal enhanced tubes. To bring the effect of mass flux and latent heat of vaporization, the Nusselt number was correlated against the product of Reynolds number and Pierre boiling number. The final correlation for Nusselt number is:

$$\mathrm{Nu} = 0.226154A(\mathrm{Re}^2\mathrm{K_f})^{0.3} \tag{12}$$

where A is the mixing parameter, which depends on number of component in the mixture. In the present work, in order to bring the effect of secondary flow inside helical coil into the Nusselt number correlation, the Dean number is replaced for Reynolds number, where Dean number is the product of Reynolds number and the ratio of centrifugal force to inertial force, which is simplified as $\mathrm{Re}(d/D)^{0.5}$. A power relation is established between the tube side heat transfer coefficient (*HTC*) and the product of Dean number and Pierre boiling number. The shell side *HTC* is correlated against the Prandtl number of the Reynolds number of agitated fluid in the bath. A power relation is established between the shell side *HTC* and the ratio of modified Reynolds number to Prandtl number of the fluid in the bath. Design Expert, a statistics software, is used to evolve the correlations.

Results and discussion

The two-phase *HTC* of any refrigerant can be directly rated using Property group [$\phi_{\mathrm{hz}}\quad k_{\mathrm{L}}^{0.6}(c_{\mathrm{pL}}/\mu_{\mathrm{L}})^{0.4}$] [13], which is derived by regrouping thermo-physical properties such as liquid viscosity, liquid thermal conductivity, and liquid specific heat capacity in the single-phase *HTC*, namely the Dittus-Boelter correlation. By applying the same method to Rogers-Mayhew correlation [19] for helical coils, the property groups for refrigerants in helical coils can be simplified ($\phi_{\mathrm{hel}}\quad k_{\mathrm{L}}^{0.6}c_{\mathrm{pL}}^{0.4}/\mu_{\mathrm{L}}^{0.45}$). The property groups of M09, R-12, R-134a, R-290, and R-600a at different pressures are compared in tab. 1. It is evident that the property group of M09 is 20-25% higher than R-12. This is because the individual components of M09 namely R-134a, R-290 and R-600a themselves have higher property group than R-12. Higher property group value is also expected to reflect in higher heat transfer coefficient of M09.

Mass flow rate of R-12 and M09 for different evaporator loads is shown in fig. 2. It is observed that the mass flow rate required for M09 is

Table 1. Operating conditions for experimentation

Pressure [bar]	R-134a	R-290	R-600a	R-12	M09
1	155.7	298.3	243.1	126.3	165.2
2	166.4	314.5	261.1	133.5	176.7
3	173.3	325.1	273.0	138.0	184.1
4	178.6	333.4	282.3	141.4	189.7

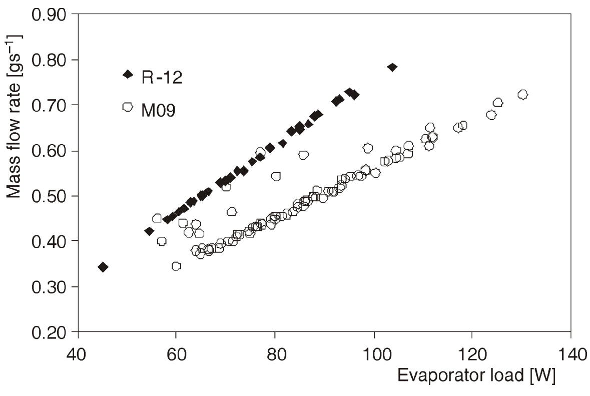

Figure 2. Influence of mass flow rate on evaporator load

Table 2. Comparison of latent heat of refrigerants

Pressure [bar]	R-134a	R-290	R-600a	R-12	M09
1	217.2	426.2	365.4	166.3	237.0
2	206.0	407.5	347.6	158.7	223.9
3	198.1	393.9	334.6	153.2	214.7
4	191.6	382.6	323.8	148.7	207.3

15-25% comparatively lesser than that of R-12 for different evaporative load. This is primarily because of higher latent heat of vaporization corresponding to a given evaporator load. The comparison of latent heat of R-12 and M09 is shown in tab. 2. The latent heat of M09 is 25-29% higher than that of R-12. Hence, it is expected that the overall two-phase (tube side) *HTC* correlation evolved from this work should incorporate dimensionless number which brings latent heat and mass flow rate, apart from the impact of helical shape. Hence, the Pierre boiling number, which incorporates the effect of latent heat, and Dean number, which brings the effect of mass flow rate in helical coil, are selected to form the correlation.

Comparison of thermo-physical properties revealed that the viscosity of the M09 and R-12 are almost same and the specific heat of M09 is 30 to 35% greater than that of R-12. Moreover, the liquid density of M09 is 17 to 20% lesser than R-12 and vapor density 27 to 30% less than R-12. Hence, the refrigerant velocity is higher for M09 than R-12 for a same mass flow rate. This is a good indication of faster convective vaporization of refrigerant inside the coil, which results in shorter coil length for a given duty, when compared to R-12. This ultimately reflects in a higher heat transfer coefficient for M09. The comparison of two-phase heat transfer coefficient in the helical coil against mass flow rate for R-12 and M09 is shown in fig. 3. The heat transfer coefficient of M09 is higher than that of R-12 and this is also evident through the higher property group values of M09. The linear slope between the mass flow rate and evaporative load is also established in the slope between mass flow rate and two-phase *HTC*. Since evaporator load and mass flow rate are directly related through latent heat of vaporization, the linear dependency of two-phase *HTC* and mass flow rate can also be related through latent heat of vaporization. Hence, it is evident that bringing Pierre boiling number in the two-phase *HTC* correlation is more appropriate.

The liquid only *HTC* inside a helical coil estimated using Rogers-Mayhew correlation is shown in fig. 4. It can be inferred from figs. 3 and 4 that both the single-phase (liquid) and two-phase mean *HTC* increase with increase in mass flow rate. Chen [27] postulated that the global heat transfer in a flow boiling process is the net effect of nucleate boiling and convective vaporization processes. In the former process, the heat transfer is predominantly due to bubble

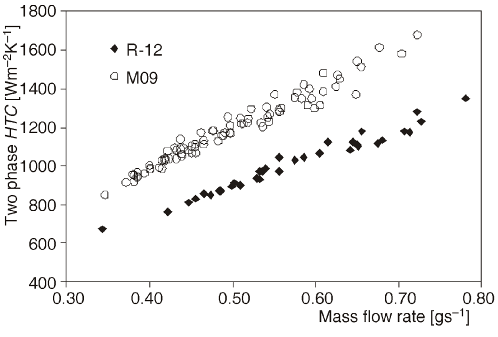

Figure 3. Influence of mean two-phase *HTC* on mass flow rate

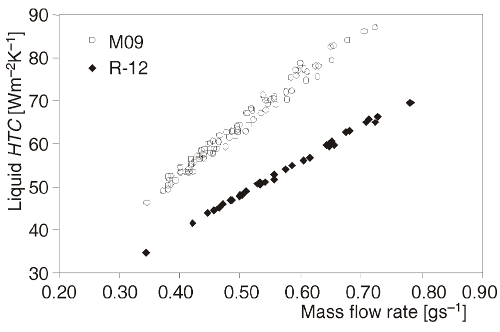

Figure 4. Influence of mean liquid *HTC* on mass flow rate

formation and the magnitude of the *HTC* is directly proportional to the heat flux. In the latter one, the heat transfer process is due to convective vaporization of liquid at the liquid-vapor interface and the *HTC* is proportional to the mass flux. It has been pointed out that nucleate boiling gets suppressed when convective vaporisation is dominant [18, 25, 26]. Aprea *et al*. [16] claimed that if nucleate boiling prevail in a flow boiling process, the trend of the mean *HTC* tend to be flat against the mass flow rate. Further, the *HTC* curve tend to be steeper for a convective dominant t process. Thus, in the present work the *HTC* is steeper and directly proportional to the mass flow rate. Thus, the convective vaporisation is the dominant process. Thus, the two-phase *HTC* can be correlated using single-phase consideration. The mean two-phase Nusselt number is correlated against the product of Reynolds number and Pierre boiling number as shown in fig. 5. The correlation predicts within deviation of 25%, shown in fig. 6 from the experimental results:

$$\text{for M09} \quad \mathrm{Nu} = 0.0096(\mathrm{DeK_f})^{0.7887} \qquad (13)$$

$$\text{for R12} \quad \mathrm{Nu} = 0.0382(\mathrm{DeK_f})^{0.658} \qquad (14)$$

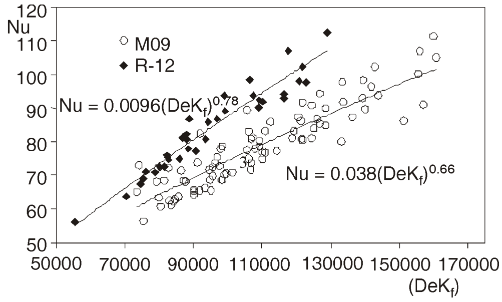

Figure 5. Correlation for the mean two-phase *HTC* using Nu, De, and K$_f$

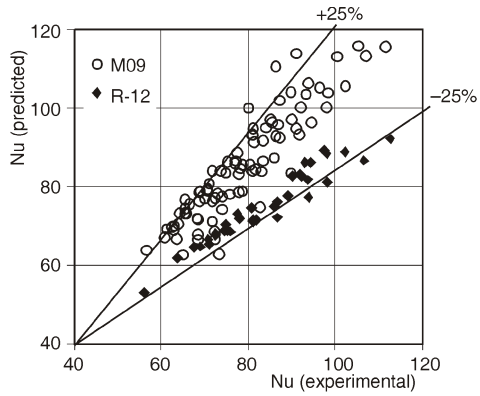

Figure 6. Deviation plot for tube-side two-phase Nusselt number

In the published literature on correlation for shell-side *HTC*, the effect of agitation is usually ignored. The effect of agitation is incorporated by using the modified Reynolds number, which is function of shell fluid property and agitator frequency [28]. Even though the frequency of the agitator is kept constant, the variation in modified Reynolds number ($\mathrm{Re_a} = d_a d_o \mathrm{N}\rho_b/\mu_b$) is realized due to the change in bath temperature. The shell side *HTC* is higher at higher ratios of $\mathrm{Re_a/Pr_b}$ and this is because the viscosity of the ethylene glycol rapidly decreases with increases in temperature and there is only a marginal decrease in density. This results in a simultaneous decrease in $\mathrm{Pr_b}$ and increase in $\mathrm{Re_a}$. The shell side *HTC* is correlated as shown in eq. 15:

$$h_{ss} \quad 50.455 \; \frac{\mathrm{Re_a}}{\mathrm{Pr_b}}^{\,0.3095} \qquad (15)$$

Conclusions

An overall heat transfer coefficient for flow boiling inside a vertical coil, for low heat and mass flux applications, is correlated for M09 against Dean number and Pierre boiling number with a deviation of ±25%. The mass flow rate required by M09 is 15-25% less than CFC12 for the same evaporative load. The *HTC* result shows that M09 is superior to CFC12 from both tube side *HTC* and as well as shell-side *HTC* point of view. This is evident from the 20-25% higher property group value of M09. The correlation is also extendable to other fluids which has similar property group. The shell side HTC correlation incorporates the effect of agitation, constant temperature bath and two-phase flow in the tube side.

Acknowledgment

The authors gratefully acknowledge the grant-in-aid provided by University Grant Commission of India (UGC).

Nomenclature

D	– helical coil diameter, [m]
De	– Dean number [= $\mathrm{Re}(d_i/D)^{1/2}$]
d	– diameter, [m]
G	– mass flux, [$\mathrm{kgs^{-1}m^{-2}}$]
h	– heat transfer coefficient, [$\mathrm{Wm^{-2}K^{-1}}$]
i	– enthalpy, [$\mathrm{Jkg^{-1}}$]
$\mathrm{K_f}$	– Pierre boiling number (= $\Delta x h_{fg}/Lg$)
k	– thermal conductivity, [$\mathrm{Wm^{-1}K^{-1}}$]
L	– length, [m]
$\dot{m}$	– mass flow rate, [$\mathrm{kgs^{-1}}$]
N	– rotation per second, [$\mathrm{s^{-1}}$]
Nu	– Nusselt number (= hD/k), [–]
Pr	– Prandtl number (= $\mu C_p/k$), [–]
p	– pressure, [Pa]
Q	– heat, [W]
q	– Heat flux, [$\mathrm{Wm^{-2}}$]
Re	– Reynolds number (= $d_a d_o N\rho_b/\mu_b$), [–]
ΔT	– superheat
t	– temperature, [K]
x	– dryness fraction

Greek letters

μ	– viscosity, [Pa·s]
ρ	– density, [$\mathrm{kgm^{-3}}$]
ϕ	– property group [$k_L^{0.6}(c_{pL}/\mu_L)^{0.4}$]

Subscripts

a	– agitator
b	– fluid bath
fg	– vaporization
g	– gas
hel	– helical
hz	– horizontal
i	– coil inside
L	– liquid
o	– coil outside
r1	– condition at inlet of the test section
r2	– condition at outlet of the test section
r2sat	– condition when x = 1
s	– multiplier factor
sh	– superheated
ss	– shell side
sup	– supplied
t	– exponent factor
tp	– two-phase
ts	– tube side
v	– superheated vapor
w	– wall

Abbreviations

CFC	– chlorofluorocarbon
HTC	– heat transfer coefficient

References

[1] ***, United Nations Environment Programme, Montreal Protocol on Substances that Deplete the Ozone Layer-Final Act, 1989

[2] Spauschus, H. O., HFC 134a as a Substitute Refrigerant for CFC 12, *Int. J. Refrigeration, 11* (1988), 6, pp. 389-392

[3] Jung, D. S., Radermacher, R., Performance Simulation of Single-Evaporator Domestic Refrigerators Charged with Pure and Mixed Refrigerants, *Int J. Refrigeration, 14* (1991), 4, pp. 223-232

[4] Carpenter, N. E., Retrofitting HFC 134a into Existing CFC 12 Systems, *Int J. Refrigeration, 15* (1992), 6, pp. 332-348

[5] Devotta, S., Gopichand, S., Comparative Assessment of HFC134a and Some Refrigerants as Alternatives to CFC12, *Int. J. Refrigeration, 15* (2) (1992), 2, pp. 112-118

[6] Jung, D., *et al*., Testing of a Hydrocarbon Mixture in Domestic Refrigerators, *ASHRAE Trans*., *19* (1996), 3, pp. 1077-1084

[7] Granryd, E., Hydrocarbons as Refrigerants – An Overview, *Int. J. Refrigeration, 24* (2001), 1, pp.15-24

[8] Fatouh, M., El Kafafy, M., Assessment of Propane/Commercial Butane Mixtures as Possible Alternatives to R134a in Domestic Refrigerators, *Energy Conversion and Management, 47* (2006), 15, pp. 2644-2658

[9] Janssen, M., Engels, F., The Use of HFC134a with Mineral Oil in Hermetic Cooling Equipment, Report 95403/NO 07, International Congress of Refrigeration, The Hague, 1995

[10] Sekhar, S. J., Lal, D. M., Renganarayanan, S., Improved Energy Efficiency for CFC Domestic Refrigerators Retrofitted with Ozone-Friendly HFC134a/HC Refrigerant Mixture, *Int. J. Thermal Sciences, 4*3 (2004), 3, pp. 307-314

[11] Sekhar, S. J., Kumar, K. S., Lal, D. M., Ozone Friendly HFC134a/HC Mixture Compatible with Mineral Oil in Refrigeration System Improves Energy Efficiency of a Walk in Cooler, *Energy Conversion and Management, 45* (2004), 3, pp.1175-1186

[12] Raja, B., Lal, D. M., Saravanan, R., Flow Boiling Heat Transfer Coefficient of R-134a/R-290/R-600a Mixture in a Smooth Horizontal Tube, *Thermal Science, 12* (2008), 3, pp. 33-44

[13] Jung, D. S., *et al.*, A Study of Flow Boiling Heat Transfer with Refrigerant Mixtures, *Int. J. of Heat and Mass Transfer, 32* (1989), 9, pp. 1751-1764

[14] Shin, J. Y., Kim, M. S., Ro, S. T., Experimental Study on Forced Convective Boiling Heat Transfer of Pure Refrigerants and Refrigerant Mixtures in a Horizontal Tube, *Int. J. Refrigeration, 20* (1997), 4, pp. 267-275

[15] Wattelet, J. P., *et al*., Evaporative Characteristics of R12, R134a and a Mixture at Low Mass Fluxes, *ASHRAE Trans. Symposia, 2* (1994), 1, pp. 603-615

[16] Aprea, C., Rossi, F., Greco, A., Experimental Evaluation of R22 and R407C Evaporative Heat Transfer Coefficient in a Vapour Compression Plant, *Int. J. Refrigeration, 23* (2000), 5, pp. 366-377

[17] Jabardo, J. M. S., Filho, E. P. B., Convective Boiling of Halocarbon Refrigerants Flowing in a Horizontal Copper Tube – an Experimental Study, *Experimental Thermal and Fluid Science, 23* (2000), 13, pp. 93-104

[18] Ali, M. E., Experimental Investigation of Natural Convection from Vertical Helical Coiled Tubes, *Int. J. Heat Mass Transfer, 37* (1994), 4, pp. 665-671

[19] Rogers, G. F. C, Mayhew, Y. R, Heat Transfer and Pressure Loss in Helically Coiled Tubes with Turbulent Flow, *Int. J. Heat Mass Trans, 7* (1964), 11, pp. 1207-1216

[20] Prabanjan, D. G., Rennie, T. J., Raghavan, G. S. V., Natural Convection Heat Transfer from Helical Coiled Tubes, *Int. J. of Thermal Sciences, 43* (2004), 4, pp. 359-365

[21] Ali, M. E., Free Convection Heat Transfer from the Outer Surface of Vertically Oriented Helical Coils in Glycerol-Water Solution, *Heat and Mass Transfer, 40* (2004), 8, pp. 615-620

[22] Jeong, S., Jeong, D., Lee, J. J., Evaporating Heat Transfer and Pressure Drop Inside Helical Coils with the Refrigerant Carbon Dioxide, *Proceedings*, 21st International Congress on Refrigeration, Washington D. C., 2003, pp. 1-6

[23] Unal, H. C., Van Gasself, M. L. G., Versalt, P. M., Dryout and Two-Phase Flow Pressure Drop in Sodium Heated Helically Coiled Steam Generators Tubes at Elevated Pressure, *Int. J. Heat Mass Transfer, 24* (1981), 2, pp. 285-298

[24] Guo, L., Feng, Z., Chen, X., An Experimental Investigation of the Frictional Pressure Drop of Steam Two-Phase Flow in Helical Coils, *Int. J. Heat Mass Transfer, 44* (2001), 14, pp. 2601-2610

[25] ***, REFPROP, NIST Standard Reference Database 23, Version 7.01, 2004

[26] Sami, S. M., Song, B., Heat Transfer and Pressure Drop Characteristics of HFC Quaternary Refrigerant Mixtures Inside Horizontal Enhanced Surface Tubing, *App. Thermal Engg., 16* (1996), 6, pp. 461-473

[27] Chen, J. C., Correlation for Boiling Heat Transfer to Saturated Fluids in Convective Flow, Industrial and Engineering Chemistry, *Process Design and Development, 5* (1966), 3, pp. 322-329

[28] Havas, G., Deak, A., Swainsky, J., Heat Transfer to Helical Coils in Agitated Vessels, *The Chem Engg J., 35* (1987), 1, pp. 61-64

Authors´ affiliations:

B. Raja
IIITD&M-Kancheepuram,
IIT Madras Campus
Chennai, India

S. J. Sekhar (**corresponding author**)
Dept. of Mechanical Engineering,
St. Xavier´s Catholic College of Engineering,
Chunkankadai, 629809, Kanyakumari District, India
E-mail: josephsekharŽhotmail.com

D. Mohan Lal
Dept of Mech. Engg.,
College of Engineering, Guindy,
Anna University, Chennai, India

Paper submitted: November 16, 2008
Paper revised: April 21, 2009
Paper accepted: April 21, 2009